J. Fluid Mech. (1965), *vol.* 22, *part* 3, *pp.* 599–615
Printed in Great Britain

Shock–shock interaction on a slender supersonic cone

By VICTOR D. BLANKENSHIP
Office of Research, Aerospace Corporation, San Bernardino, California

(Received 15 October 1964 and in revised form 4 January 1965)

The transient pressure field produced behind a plane shock wave of arbitrary strength, which encounters a slender supersonic cone head on, is theoretically predicted. The analysis is restricted to small cone angles (in order that Mach-reflexion will occur at the surface) and to inviscid flow.

A conical-flow technique is utilized to transform the small-perturbation equations of time-dependent rotational motion of the fluid behind the deflected plane shock into time-independent equations. From these equations, a boundary-value problem for pressure alone, in the Mach-reflexion region, is derived which is solved numerically. Results for the small perturbation pressure field of the cone are contrasted with Smyrl's (1963) results, which hold for a moving wedge, for a range of values of cone and plane shock speeds.

1. Introduction

This paper defines the magnitude and nature of the aerodynamic loading associated with the interaction between a blast wave and a slender supersonic cone. The problem has practical importance from the viewpoint of both weapon analysis and the vulnerability of either a missile or a re-entry vehicle to a nuclear blast. To date, no experimental or analytical results have been reported which elucidate this problem. The physical problem is that of a blast wave, which is considered to be a plane shock wave, meeting a slender cone which is moving in the opposite direction at supersonic speed. The plane shock is considered to be of arbitrary strength, and the supersonic cone is considered to have an attached shock.

This work utilizes an approach similar to that used in the earlier work by Lighthill (1949) and Smyrl (1963). Lighthill considered the behaviour of an arbitrary-strength, plane shock wave moving along a wall and meeting a corner of small angle which is at rest relative to the surrounding air. When the corner is convex, pure diffraction occurs. At a concave corner Mach reflexion occurs; this case corresponds to a plane shock wave meeting normally a thin infinite wedge at rest. Chester (1954) extended the problem of Lighthill to the case of infinite wedges at yaw. Ehlers & Shoemaker (1959) furnished a solution for the linearized interaction between a weak shock wave and a moving half plane. Smyrl (1963) extended the work of Chester and Lighthill by finding the pressure field in closed analytic form for the region behind an arbitrary-strength shock wave which has encountered a thin airfoil moving at supersonic speed. His solution is valid

for wedges at small incidence to the free-stream flow and for wedges yawed with respect to the shock plane. He also extended the solution to include the case of a thin airfoil of arbitrary shape.

Whitham (1957, 1958, 1959) developed an approximate theory for the prediction of shock patterns associated with the interaction of a blast wave with two- and three-dimensional stationary bodies. Bryson & Gross (1961) experimentally investigated the diffraction of plane strong shocks by several cones, a cylinder and a sphere. The diffraction pattern, in particular, the shape of the diffracted shocks, and the loci of the Mach triple points, compared favourably with the theoretical results obtained by Whitham. Whitham's technique is based only on kinematical considerations and does not analyse the pressure distribution. Miles (1963) attempted some preliminary calculations on the adaptation of Whitham's technique to a moving body, utilizing the configuration employed by Smyrl, but these calculations yielded unsatisfactory results. Miles later (1964) obtained qualitatively satisfactory results.

Ting & Ludloff (1952) treated the problem of a blast passing over the surface of a stationary arbitrary two-dimensional structure and were able to present the pressure and density fields in the whole domain behind the advancing blast in explicit analytic form. Ludloff & Friedman (1952) treated the problem of a strong blast passing over a stationary axially symmetric cone by a modification of the procedure of Ting & Ludloff. In both these approaches, hyperbolic equations were used throughout.

2. Flow regions

The problem under consideration (figure 1) is that of axially symmetric diffraction of a plane strong shock by a Mach wave (weak shock) attached to the tip of the cone. The plane shock, the plane of which coincides at time $t = 0$ with the (R, Z)-plane, moves with supersonic velocity U in the X-direction into a region (0) of still air; the air behind the shock has a velocity of V_1. A slender axially symmetric cone of infinite length, whose tip at $t = 0$ also coincides with the (R, Z)-plane, moves with supersonic speed W in the negative X-direction. When $t \leqslant 0$ the flow regions are (0), (1) and (2); regions (0) and (1) are uniform and are separated by the plane shock of arbitrary strength, while region (0) is separated from the spatially non-uniform region (2) by a Mach wave emanating from the apex of the slender cone of semi-apex angle ϵ. A solution is sought for the time domain of interest $t > 0$.

For $t > 0$, the flow regions are indicated in figure 1. Smyrl (1963) postulated a form for the interaction region with the aid of a shallow water experiment for the case of a moving slender wedge. Weak attached shocks are treated for both the wedge and cone cases, and therefore the configuration of the interaction region developed by Smyrl (1963) is adopted here. Physical arguments for this configuration are given below.

The penetration of the slender cone past the plane shock and into the uniform flow behind it causes a slight disturbance of that otherwise undisturbed flow. This slight disturbance creates several flow regions (3), (4), (5), (6) and the

Mach-reflexion region shown in figure 1. These flow regions are consequently treated as small perturbations of region (1). The following idealizations apply to figure 2.

(1) The plane shock is deflected at point I, having interacted with the weak shock originally attached to the apex of the cone. The diffracted plane shock is only slightly deflected from the undiffracted position and it intersects the cone

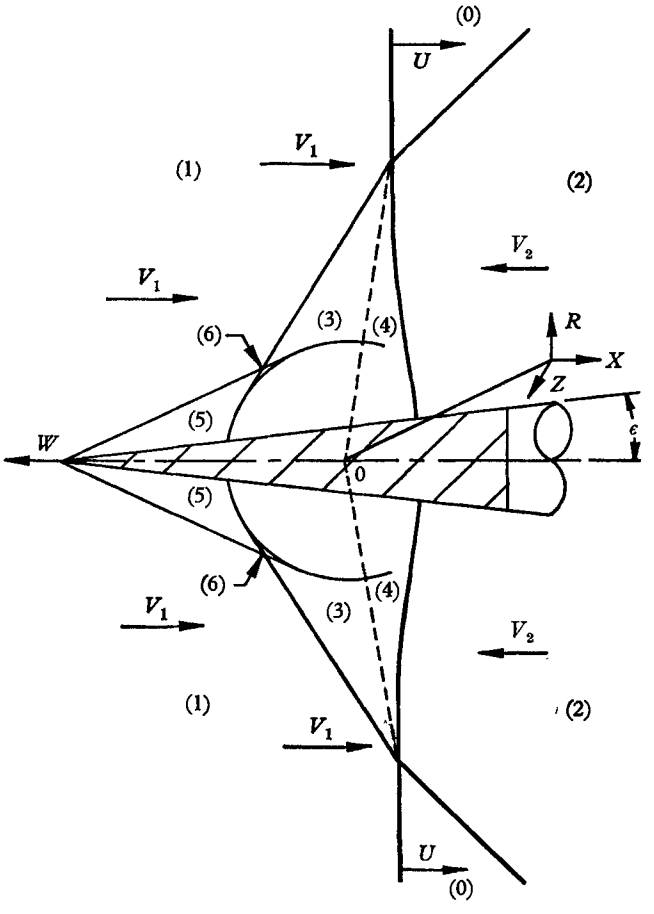

FIGURE 1. The three-dimensional interaction.

surface normally. This normal condition is necessary so that the flow behind the shock will remain parallel to the surface.

(2) The weak shock is deflected at I into the position of the tangent IC to the wave $EDCB$. In addition, a new weak shock AD is formed tangent to this wave and attached at the apex to form region (5).

(3) It should be noted that the contact discontinuity IO must move with the particle velocity so that it is located approximately as shown in figure 2. IO divides the air into two non-mixing regions (3) and (4), thus separating the flow which comes from region (2) from that which initially comes from region (0).

(4) The flow is considered to be inviscid.

With regard to the flow pattern of figure 2, region (2) is now truncated but otherwise not affected by the traversing shock and therefore time-independent solutions apply. Since weak waves are being treated, the form of the Mach-reflexion region or unsteady disturbance, according to Huyghens' principle, is that of a spherical wavelet. The radius of the disturbance is $C_1 t$, since it is known that this disturbance will be spread at the local speed of sound C_1 relative to the local fluid velocity. This disturbance is being propagated away from the tip in the positive X-direction at a velocity $(W + V_1)$. In region (5), the flow has been created by the forward part of the cone, and, since $C_1 < (W + V_1)$, the spread

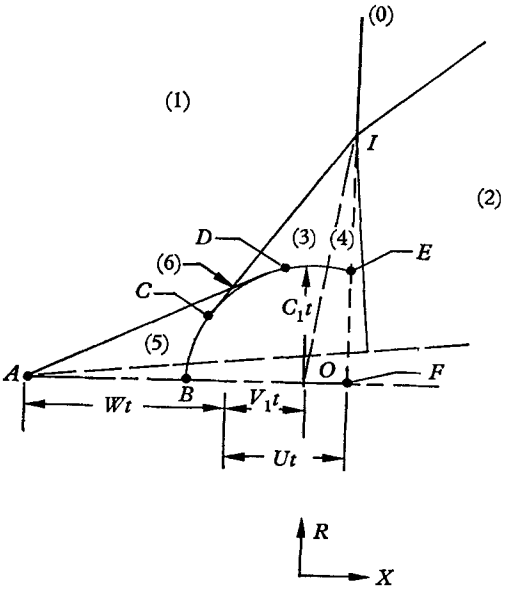

FIGURE 2. Flow regions for $t > 0$.

of the disturbance is unable to propagate back to the tip; therefore time-independent solutions for cones apply to this region. The weak shock AD is attached to the tip of the cone, and the fluid passing through this bow wave has a supersonic velocity with respect to the cone. Consequently, there will be a region of supersonic flow, region (5), separated from the Mach-reflexion region by the sector BD of the Mach circle in figure 2. Steady-flow equations also apply to regions (3) and (4), but only with respect to a frame of reference fixed to the flow in region (1).

In view of the assumed flow, the co-ordinate system is placed $(U - V_1)t$ behind the undeflected plane shock in the Mach-reflexion region. It should be noted that the pressure on the cone surface in this region influences the speed and deflexion of the curve shock. On the other hand, the change in speed and deflexion also changes the pressure.

Since the small perturbation is based on region (1) alone, the plane shock

wave is not restricted in strength, and the conservation equations applied across the shock, with the Mach number $M = U/C_0$, yield

$$\left.\begin{aligned} &\frac{\rho_1}{\rho_0} = \frac{(\gamma+1)M^2}{(\gamma-1)M^2+2}, \qquad \frac{P_1}{P_0} = \frac{2\gamma M^2-(\gamma-1)}{\gamma+1}, \\ &\frac{C_1}{C_0} = \left(\frac{P_1}{P_0}\frac{\rho_0}{\rho_1}\right)^{\frac{1}{2}}, \qquad M_1 = \frac{V_1}{C_1} = \left(\frac{2}{\gamma+1}\right)\left(\frac{C_0}{C_1}\right)\left(1-\frac{1}{M^2}\right)M, \end{aligned}\right\} \tag{1}$$

where the subscripts correspond to the particular flow regions (1) and (0).

The Mach number of the cone is $M' = W/C_0$. For the present discussion the origin is on the apex, point A of figure 2. The physical constants defining this problem are W, U, P_0, ρ_0 and ϵ. The physical constants cannot be arranged to yield a fundamental length or time-scale defining the problem. Therefore each physical quantity is a function of only X/t or R/t and the number of independent variables may be reduced. The flow field is a 'conical field' which Busemann (1943) first discussed in the study of three-dimensional steady supersonic flow. Regions (2) and (5) are clearly conical since velocity vectors along any line emanating from the apex of the cone are constant, being dependent only upon angle. The other regions are such that figure 1 will simply be magnified linearly with time.

3. Mach-reflexion region

The Mach-reflexion region, the unsteady region discussed in the previous section, is governed by the equations of unsteady inviscid, rotational motion. The rotationality is due to the curvature of the deflected plane shock from I down to the surface of the cone (figure 2). These equations, where $\mathbf{V}$, P, and ρ are the velocity vector, pressure and density respectively, are

$$\left.\begin{aligned} &\frac{\partial\rho}{\partial t} + \nabla.(\rho\mathbf{V}) = 0, \\ &\frac{\partial\mathbf{V}}{\partial t} + (\mathbf{V}.\nabla)\mathbf{V} = -\frac{1}{\rho}\nabla P, \\ &\frac{\partial}{\partial t}(P\rho^{-\gamma}) + (\mathbf{V}.\nabla)(P\rho^{-\gamma}) = 0. \end{aligned}\right\} \tag{2}$$

The linearization of equations (2) is accomplished by considering the flow in the Mach-reflexion region and regions (3), (4), (5) and (6) as slightly perturbed from region (1). For the Mach-reflexion region the small perturbation is time dependent, and Taylor expansions are taken in powers of ϵ^2 (Courant & Friedrichs 1948):

$$\left.\begin{aligned} P &= P_1 + \epsilon^2\rho_1 C_1^2 P'(X,R,t) + \ldots, \\ \rho &= \rho_1 + \epsilon^2\rho_1\rho'(X,R,t) + \ldots, \\ \mathbf{V} &= \epsilon^2 C_1\mathbf{V}'(X,R,t) + \ldots. \end{aligned}\right\} \tag{3}$$

The subscript 1 pertains to the flow in region (1) and P', ρ', and $\mathbf{V}'$ are non-dimensional.

The position of the diffracted plane shock is given by

$$X = (U - V_1)t + \epsilon^2 F(X, R, t) + O(\epsilon^4). \tag{4}$$

The boundary of the Mach-reflexion region, the Mach circle for a small perturbation to order ϵ^2, is the spherical wavelet. The spread of this disturbance is given explicitly by

$$(X^2 + R^2)^{\frac{1}{2}} = C_1 t + \epsilon^2 G(X, R, t) + O(\epsilon^4). \tag{5}$$

However, for consistency in the linearization, boundary conditions are specified only at $X = (U - V_1)t$ and $(X^2 + R^2)^{\frac{1}{2}} = C_1 t$. Therefore, it is seen that the disturbance is described by the sphere

$$X^2 + R^2 = (C_1 t)^2. \tag{6}$$

The number of independent variables of the governing equations (2) is reduced to two by means of a conical transformation (Lighthill 1949) which makes the problem time independent. The transformations are

$$x = X/C_1 t, \quad r = R/C_1 t. \tag{7}$$

The transformation yields

$$\left.\begin{aligned} &\frac{\partial}{\partial X} = \frac{1}{C_1 t}\frac{\partial}{\partial x}, \quad \frac{\partial}{\partial R} = \frac{1}{C_1 t}\frac{\partial}{\partial r}, \quad \nabla = \frac{1}{C_1 t}\nabla', \\ \text{and} \quad &\frac{\partial}{\partial t} = \frac{-x}{t}\frac{\partial}{\partial x} - \frac{r}{t}\frac{\partial}{\partial r} = -\frac{1}{t}\mathbf{S}.\nabla'. \end{aligned}\right\} \tag{8}$$

In the above equation, $\mathbf{S}$ is the length vector with components $\{x, r\}$. Therefore the non-linear equations (2) transform to

$$\left.\begin{aligned} &(\mathbf{S}.\nabla')\rho - \frac{1}{C_1}\nabla'.(\rho\mathbf{V}) = 0, \\ &(\mathbf{S}.\nabla')\mathbf{V} - \frac{1}{C_1}(\mathbf{V}.\nabla)\mathbf{V} = \frac{1}{\rho C_1}\nabla' P, \\ &(\mathbf{S}.\nabla')(P\rho^{-\gamma}) - \frac{1}{C_1}(\mathbf{V}.\nabla')(P\rho^{-\gamma}) = 0. \end{aligned}\right\} \tag{9}$$

Substituting equations (3) into equations (9) and retaining terms with coefficient of ϵ^2 alone, there result the following linear equations:

$$\left.\begin{aligned} &(\mathbf{S}.\nabla')\rho' = \nabla'.\mathbf{V}', \\ &(\mathbf{S}.\nabla')\mathbf{V}' = \nabla' P', \\ &(\mathbf{S}.\nabla')P' = (\mathbf{S}.\nabla')\rho'. \end{aligned}\right\} \tag{10}$$

Equation (10) may be algebraically manipulated to eliminate the components u' and v' of V'. This reduction results in a second-order partial differential equation in pressure alone which is

$$\frac{\partial^2 P'}{\partial r^2} + \frac{1}{r}\frac{\partial P'}{\partial r} + \frac{\partial^2 P'}{\partial x^2} = \left(r\frac{\partial}{\partial r} + x\frac{\partial}{\partial x} + 1\right)\left(r\frac{\partial P'}{\partial r} + x\frac{\partial P'}{\partial x}\right). \tag{11}$$

The problem remaining is to solve the above elliptic boundary-value problem with the appropriate boundary conditions, which is the subject of the next section.

For the cases of the stationary wedge (Lighthill 1949) and the moving wedge (Smyrl 1963), a differential equation is found which is quite similar to (11). The difference is in the second term on the right-hand side of (11). For the equation without that term, Busemann (1943) showed that it can be transformed into Laplace's equation. This technique was employed by both Lighthill and Smyrl in their analyses. A similar type of transformation for (11) was not found.

The question of rotationality is now discussed. In figure 2, the flow inside *IOF* is rotational whereas it is irrotational outside. Since the Mach circle is given by equation (6), shocks *AD* and *IC* are Mach waves, and small perturbation theory is used. Particles do not acquire vorticity by crossing these shocks but only by crossing the curved portion of the incident diffracted plane shock. These particles with vorticity stay inside *IOF*. Also, as pointed out by Smyrl (1963), the contact discontinuity does not appear in the boundary-value problem for P'. Ting & Ludloff (1952), for the stationary wedge, showed there is no discontinuity of density in a mathematical sense, but in the physical sense there is a slip-stream of finite width. Ludloff & Friedman (1952), for the stationary cone, showed that the difference of the entropy changes across the incident and Mach shocks is not supplied by a narrow slip-stream, but by an entropy gradient spread uniformly over the domain between the diffracted shock and the contact surface. It can be shown, in the manner of Smyrl, that P' of (11) can be solved without regard for the contact surface.

4. Boundary conditions

On the circular arc and straight line of *BCDEF*, enclosing the Mach reflexion region, the boundary conditions for P' vary continuously for the different flow regions. The points lying on this line are given by the following transformed conical co-ordinates:

$$\left.\begin{aligned}
x_0 &= C_0/C_1 M - M_1,\\
x_1 &= -(M_1 + M' C_0/C_1)^{-1},\\
\lambda_2 &= \{M'^2 - 1\}^{\frac{1}{2}},\\
r_3 &= (C_0/C_1)\,(M' + M)/\lambda_2,\\
x_2 &= -\{r_3(x_0^2 + r_3^2 - 1)^{\frac{1}{2}} - x_0\}/(x_0^2 + r_3^2),\\
r_i &= (1 - x_i^2)^{\frac{1}{2}} \quad (i = 0, 1, 2),\\
x_4 &= x_0/(x_0^2 + r_3^2)^{\frac{1}{2}},\\
r_4 &= r_3/(x_0^2 + r_3^2)^{\frac{1}{2}},
\end{aligned}\right\} \tag{12}$$

The co-ordinates of the letters in figure 2 are B, $(-1, 0)$; C, (x_2, r_2); D, (x_1, r_1); E, (x_0, r_0); F, $(x_0, 0)$.

In the following discussion P'_i indicates the non-dimensional perturbed pressure in the flow region (i). The pressure P'_6, if it exists, is simply $P'_5 + P'_3$ since the flow regions have been linearized and the pressures are therefore additive. If $r_1 < r_2$, then the value of P'_6 is identically zero since region (6) disappears.

For region (5), the small perturbations on the unit arc from B to D if $r_1 \leqslant r_2$ or B to C if $r_1 > r_2$ according to Liepmann & Roshko (1956) are:

$$\left.\begin{aligned} \lambda_5 &= \{(M'C_0/C_1 + M_1)^2 - 1\}^{\frac{1}{2}}, \\ u'_5 &= -(M'C_0/C_1 + M_1)\cosh^{-1}\{(M'C_0/C_1 + M_1 + x)/(\lambda_5 r)\}, \\ v'_5 &= (M'C_0/C_1 + M_1)\lambda_5[\{(M'C_0/C_1 + M_1 + x)/(\lambda_5 r)\}^2 - 1]^{\frac{1}{2}}, \\ P'_5 &= -(M'C_0/C_1 + M_1)u'_5. \end{aligned}\right\} \tag{13}$$

The limitations on this linearization are

$$\left.\begin{aligned} &\cot\epsilon \gg \lambda_5, \\ &\tan\epsilon \cosh^{-1}\left[\frac{\cot\epsilon}{\lambda_5}\right] \to 0, \\ \text{or} \quad &\epsilon\lambda_5 \ll 1, \end{aligned}\right\} \tag{14}$$

which provides for only infinitely weak, conical shock waves whose inclination is exclusively dependent upon $\{M'C_0/C_1 + M_1\}$. This limitation applies to the entire analysis.

The boundary conditions on the unit arc from regions (3) and (4) and at $x = x_0$ are considered next. An essential difficulty in this problem is the determination of the amount of deflexion of the plane shock. Lighthill (1949) and later Smyrl (1963) were able to derive a differential boundary condition, relating the normal and tangential derivatives, at the undeflected plane shock location. A similar attempt was made here which proved to be unfruitful. Also, for the wedge, regions (3) and (4) have constant values of perturbed pressures and velocities with the result that it is possible to determine them completely in terms of the deflexion of the plane shock. For the slender cone, regions (3) and (4) have spatially non-uniform perturbed pressures and velocities, and the above method does not apply.

To obtain the boundary condition at $x = x_0$, one lets the position of the shock front be given by $x = x_0 + \epsilon^2 f(r) + O(\epsilon^4) + \ldots$ in a manner similar to that of Lighthill (1949). The $\epsilon^2 f(r)$ is uniformly small when ϵ^2 is small. The portion of the shock wave between I and F is distorted to an order of magnitude consistent with the perturbation. The conditions behind the diffracted shock are dependent on the local velocity of the shock normal to itself. The shock relations are such that those terms of order ϵ^0 are the customary normal shock condition. For the wedge the terms of order ϵ provide a differential boundary condition, but not for the cone. As shown below a different approach is used.

In order to arrive at boundary conditions for regions (3) and (4) and at $x = x_0$, it is first necessary to outline a procedure that was originally privately suggested by Busemann in 1964 to the author. Historically accredited by Busemann to H. Weyl, it is related to the method by which two-dimensional interferometer photographs of three-dimensional phenomena were interpreted. Since it does not appear to be adequately discussed in the literature the approach is given here in detail.

In the following $P'_i(x, r)$ is defined as before. First a brief outline of the development without details is given, and then the detailed outline is given. A function

$P'_B(x,y)$ is found by integrating $P'_i(x,r)$. An artificial function $P_c(x,r)$ is found by integrating $P'_B(x,y)$. Evaluation of the last two steps yields $P_c(x,r)$ to be the integral of $P'_i(x,r)$. Differentiation of $P_c(x,r)$ yields therefore $P'_i(x,r)$. Now $P'_B(x,y)$ may also be found independently by integrating P'_{iw}, the known wedge distribution, where the *iw* designates the corresponding flow region (*i*) of the wedge and then $P_c(x,r)$. Therefore, $P'_i(x,r)$ can be determined from the known $P'_{iw}(x,y)$.

$P'_B(x,y)$ is taken as the two-dimensional description of a pressure field found by integrating $P'_i(x,r)$ distributions along the z-co-ordinate from $-\infty$ to $+\infty$ for a fixed y. Therefore, a linear integral equation arises which can be written in the final form

$$P'_B(x,y) = \int_{-\infty}^{+\infty} P'_i[x,(y^2+z^2)^{\frac{1}{2}}]\,dz = 2\int_{R=y}^{\infty} P'_i(x,R)\,\frac{R}{(R^2-y^2)^{\frac{1}{2}}}\,dR. \tag{15}$$

If $P'_B(x,y)$ were known, then with the kernel, $R(R^2-y^2)^{-\frac{1}{2}}$, equation (15) is a Volterra integral equation of the first kind. The $P'_B(x,y)$ physically describes the two-dimensional pressure field of a supersonic flow on a concave aerofoil. The problem, therefore, is to provide a separate description of $P'_B(x,y)$ and, in addition, provide an inversion or its equivalence of equation (15) to provide $P'_i(x,r)$.

The $P'_B(x,y)$ distribution with the linearly increasing slope of its surface can be replaced, using superposition, by a linear succession of wedges of given constant angle. Considering the conical character of both the wedge and cone interaction problems, one recognizes that the flow regions are similar about $r=0$ and $x=x_0$ of figure 2. For the wedge, this point of similarity was noted by Smyrl (1963) in the section on an aerofoil of arbitrary shape. The pressure distribution from each individual wedge is the same except for size with respect to the others; see Smyrl's figure 12. The individual contributions to the pressure $P'_B(x,y)$ on a space-fixed point (x,y), referenced to $(x_0,0)$, are found on the relative co-ordinates $(x/\omega,\ y/\omega)$, where ω is the ratio of the tip penetration of succeeding wedges with respect to its value on the starting wedge. Therefore, the pressure integral, for a linear succession of wedges, reads as follows:

$$P'_B(x,y) = K\int_0^1 P'_{iw}(x/\omega, y/\omega)\,d\omega, \tag{16}$$

where K is a constant. $P'_{iw}(x,y)$ is the two-dimensional pressure distribution for a wedge.

There is still needed an inversion, or its equivalence, of equation (15). $P'_B(x,y)$ is rotated 360°, and integration is performed for a fixed r along ϕ from $-\infty$ to $+\infty$, where $y=(r^2+\phi^2)^{\frac{1}{2}}$ ($y\,dy=\phi\,d\phi$). The resulting new function $P_c(x,r)$ is given by

$$P_c(x,r) = \int_{-\infty}^{+\infty} P'_B[x,(r^2+\phi^2)^{\frac{1}{2}}]\,d\phi = 2\int_{y=r}^{\infty} P'_B(x,y)\,\frac{y}{(y^2-r^2)^{\frac{1}{2}}}\,dy. \tag{17}$$

Substitution of (15) into (17) yields

$$P_c(x,r) = 4\int_{y=r}^{\infty}\left[\int_{R=y}^{\infty} P'_i(x,R)\,\frac{R}{(R^2-y^2)^{\frac{1}{2}}}\,dR\right]\frac{y}{(y^2-r^2)^{\frac{1}{2}}}\,dy. \tag{18}$$

Simplification of (18) yields

$$P_c(x,r) = 2\pi\int_r^{\infty} P'_i(x,R)\,R\,dR. \tag{19}$$

The equivalence of an inversion, by differentiation of (19), yields

$$P'_i(x,r) = -\frac{1}{2\pi r}\frac{\partial P_c}{\partial r}. \tag{20}$$

The method of applying (16)–(20) to obtain the perturbed pressure distribution is as follows: First (16) is used with the values of P'_{iw} obtained from the theory of the wedge case by Smyrl. Secondly, $P_c(x,r)$ is determined by integration. The desired $P'_i(x,r)$ can then be found from (20). This method and order of steps are used to calculate boundary values on the Mach circle, from C to E for P'_3, and E to F for P'_4. The reason the entire Mach-reflexion region, rather than just its boundary conditions, is not worked in this manner is that the method becomes quite involved numerically.

As an example of this procedure, first consider the boundary values of P'_4 behind the shock for $x = x_0$ and $r_0 < r \leqslant r_3$. The P'_{4w} in equation (21) is the constant value for the wedge in region (4) (Smyrl 1963). After completion of the trivial analytical steps, P'_4 becomes

$$P'_4(x,r) = \frac{P'_{4w}}{T_0}\cosh^{-1}(r_3/r), \tag{21}$$

where $T_0 = [M'^2 - 1]^{\frac{1}{2}}$. Using (21) and the fact that regions (3) and (4) are conical and supersonic, one can obtain the boundary condition on the unit arc.

For the larger range of independent variable r, $0 < r < r_3$ and $x = x_0$, it is necessary in order to delineate the steps first to compute, by means of (16), the following function numerically:

$$P'_B(x_0,y) = K\int_0^1 P'_{iw}(x_0/\omega, y/\omega)\,d\omega, \tag{22}$$

where the P'_w stands for the wedge value. This result is substituted into (17) and it yields

$$P_c(x_0,r) = 2\int_r^{r_3} P'_B(x_0 y)\frac{y}{(y^2-r^2)^{\frac{1}{2}}}dy.$$

The final step, equation (17), results, for the range $0 < r \leqslant r_3$ and $x = x_0$, in

$$P'(x_0,r) = -\frac{1}{2r}\frac{\partial}{\partial r}(P_c(x_0,r)). \tag{23}$$

Some results of these numerical calculations are presented in table 1.

It should be noted that application of the above procedure to steady flow results in a neglect of the v'^2 contribution to the pressure coefficient. Since this method is used to calculate boundary conditions at $x = x_0$ and the boundary of regions (3), (4), and (6), if it exists, then for region (5) the contribution of v'^2 to P'_5 is consistently neglected, as can be seen in (13). The completely correct approximation for P'_5 (Liepmann & Roshko 1956) is

$$P'_5(x,r) = -u'_5(M'C_0/C_1 + M_1) - \tfrac{1}{2}\epsilon^2 v'^2_5. \tag{24}$$

The last term is negligible everywhere except in the vicinity of the cone surface, where the order of v' is different from u'. Equation (24) at the cone surface is

$$P'_5(x,r) = [M'C_0/C_1 + M_1]^2\{\log_e(2/\lambda_5\epsilon) - \tfrac{1}{2}\} = [M'C_0/C_1 + M_1]^2\log_e(2/\lambda_5\epsilon). \tag{25}$$

The approximation of (25) is valid if

$$\log_e(2/\lambda_5\epsilon) \gg \tfrac{1}{2} \quad \text{or} \quad \lambda_5\epsilon \ll 1, \tag{26}$$

which are the criteria of (14) and no new limitation is required.

Boundary values have been described from B to F with only the boundary along the axis from F to B remaining to be determined. Owing to the singularities on the axis, it is necessary to formulate the boundary conditions on the surface in the following manner.

The shape of an axially symmetric body is determined by h, which represents the cross-sectional radius of the body. The boundary condition along the surface is that the normal velocity vanishes. This boundary condition requires

$$\frac{v'}{M'C_0/C_1+M_1+\epsilon'u'} = h' \doteq \frac{v'}{M'C_0/C_1+M_1}, \tag{27}$$

where the h' indicates differentiation of h. For an axially symmetric body the expression $v'R/(M'C_0/C_1+M_1)$ is equal to hh'. As an approximation, therefore, one may take

$$v'R = (M'C_0/C_1+M_1)\,hh', \tag{28}$$

which says that $v'R$ is essentially a constant in the vicinity of the axis.

Therefore, on the surface it is

$$\left.\begin{aligned} &v'R\{x < (MC_0/C_1-M_1), r \to 0, t\} = (M'C_0/C_1+M_1)\,hh', \\ \text{where} \quad &h = h[X+(M'C_0/C_1)+M_1)\,C_1t]. \end{aligned}\right\} \tag{29}$$

Using the perturbed, non-transformed r-momentum equation

$$\frac{\partial P'}{\partial R} = -\frac{1}{C_1}\frac{\partial v'}{\partial t},$$

there results the following equation:

$$R\,\partial P'/\partial R = -(M'C_0/C_1+M_1)^2[h'^2+hh''']. \tag{30}$$

Because $h''' = 0$, the boundary condition on the surface of the cone in conical co-ordinates is

$$r\,\partial P'/\partial r = -(M'C_0/C_1+M_1)^2. \tag{31}$$

Equation (31) can also be obtained from the transformed r-momentum equation found in (10). To check the continuity of this derivative one has only to investigate P_5'. Its derivative is found to be the same as (31) in the neighbourhood of B.

When $r_3 < r_0$, the interaction is inside the sonic circle. This phenomenon can be seen in figure 3. There are, therefore, no regions (3) and (4). The interaction point I still consists, however, of three shocks and a contact discontinuity. The contact discontinuity is considered to be approximately in the location of a straight line from the origin to r_3. This particular case is not treated here.

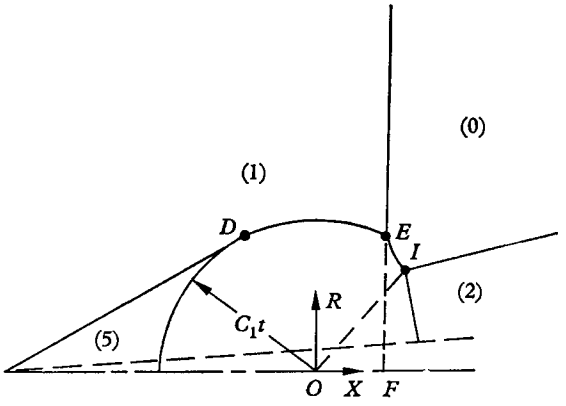

FIGURE 3. Flow regions for $t > 0$, $r_3 < r_0$.

5. Method of solution

Inspection of the variable coefficients of (11) shows that inside the Mach circle the partial-differential equation is elliptic; physically it is a subsonic region. At the boundary it is parabolic. Outside the Mach circle the equation is hyperbolic. A closed form solution of the elliptic region appears not possible so numerical methods were used. The boundary conditions are mixed, since both Dirichlet and Neumann types appear.

A finite-difference-equation analogue of (11) was constructed on a square mesh, where each computational unit was composed of nine grid points of mesh spacing equal to 0·025 compared to a maximum Mach circle radius of 1·0, by replacing partial derivatives with certain partial difference quotients (see Forsythe & Wasow 1960). The resulting system of linear equations was solved iteratively by the method of successive over-relaxation and employed a relaxation factor to accelerate convergence. This iterative process was repeated cyclically until a relative residual was found to be less than 10^{-6}. The maximum normalized residual $m^{(n)}$, where n is the nth iterate, of the above criteria was found to be

$$m^{(n)} = \frac{\max|P^{(n)} - P^{(n-1)}|}{P^{(n)}} < 10^{-5}$$

for all cases.

6. Discussion of results

The pressure distribution has been calculated in a number of cases at the surface of the cone. The perturbed-surface-pressure variation in the Mach-reflexion region from B to F is illustrated in figure 4. The distance from B to F is adjusted to make it the same for all cases. For two of the cases shown in figure 4, the perturbed pressure behind the traversing shock wave, $x = x_0$, exceeds the new steady-state surface pressure P_5' of the cone at $x = -1$. The pressure variation is practically linear. This is due to the fact that in the neighbourhood of F, at the cone surface, the slope of the pressure is continuous and the pressure tends to remain constant for some distance along the surface. Compared to the wedge case (Smyrl 1963) the behaviour is different because in the cone case boundary

condition (31) governs, whereas the derivative of perturbed pressure is equal to zero for the wedge on the axis. The isobars in the two cases reflect the basic difference. The angle of the cone has been restricted to small values to minimize the parameter ϵ. The above-mentioned pressure ratio will be discussed below.

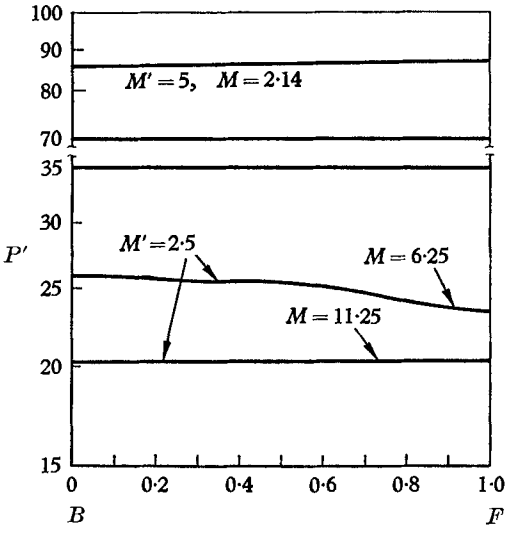

FIGURE 4. Pressure variation on the cone surface.

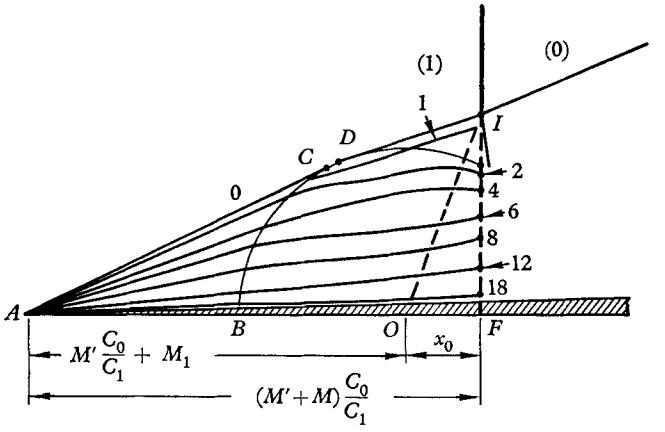

FIGURE 5. The pressure distribution for $M = 11{\cdot}25$, $M' = 2{\cdot}5$, $\epsilon = 0{\cdot}025$.
———, Isobars $(P - P_1)/\rho_1 C_1^2 \epsilon^2$.

Figure 5 illustrates the total pressure field over the entire region for a particular case. Figure 5 is more easily clarified by also reviewing figure 2. The origin of the sonic circle after the blast shock has collided with the tip of the cone, i.e. for $t > 0$, is at a dimensionless distance $(M'C_0/C_1 + M_1)$ measured downstream from the tip. The plane shock is at a distance $(M' + M)\, C_0/C_1$ also measured downstream from the tip. The radius of the Mach circle is normalized to be 1. The isobars of the steady conical flow of region (5) are to the left of the sonic circle and serve as its boundary conditions. The isobaric distributions of the Mach-reflexion

region, interposed between regions (5) and (2), are illustrated in figures 6 and 7 for two distinct cases. It is interesting to note the extent to which the conical character of region (5) extends into the disturbed region.

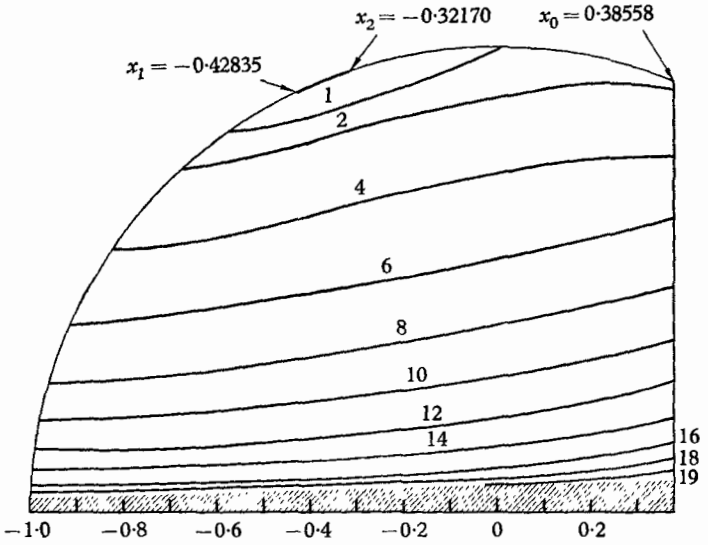

FIGURE 6. Transient isobars for $M = 11{\cdot}25$, $M' = 2{\cdot}5$, $\epsilon = 0{\cdot}025$.

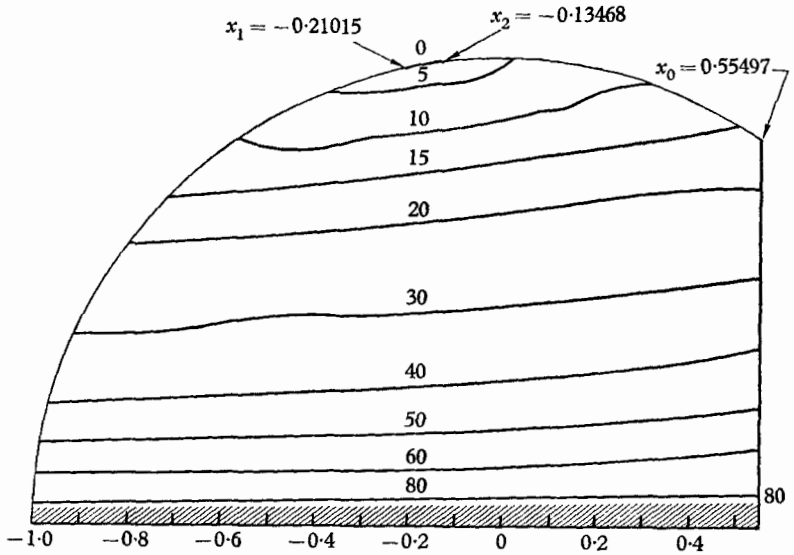

FIGURE 7. Transient isobars for $M = 2{\cdot}14$, $M' = 5$, $\epsilon = 0{\cdot}01$.

The transient pressure distribution is transmitted to the cone surface in the following manner. For example, a particular point is at a distance L from the leading tip and at $t = 0$ the shock wave strikes the tip of the cone. Therefore at $t = L/(C_0 M' + C_0 M)$ the point will experience a new pressure change due to the transmitted shock and subsequently feel the surface pressure distribution inside the Mach circle. When $t = L/\{C_0(M' + M) - C_1\}$, a new steady-state condition

will prevail, and the pressure will be constant from that point back to the tip. The duration of the transient phase is therefore

$$\Delta t = \frac{L/C_0}{\{C_0/C_1(M'+M)-1\}\{M'+M\}}. \tag{32}$$

For example, if $M' = 3$, $M = 5$ and $C_0 = 1000$ ft./sec, the duration of the transient phase for $L = 1$ is 50 μsec.

Figures 6 and 7 illustrate the pressure field on and above the surface of the cone. Figures 5, 6 and 7 have to be rotated 360 degrees about the axis of symmetry for the physical picture. The Mach-reflexion region is viewed as a sphere

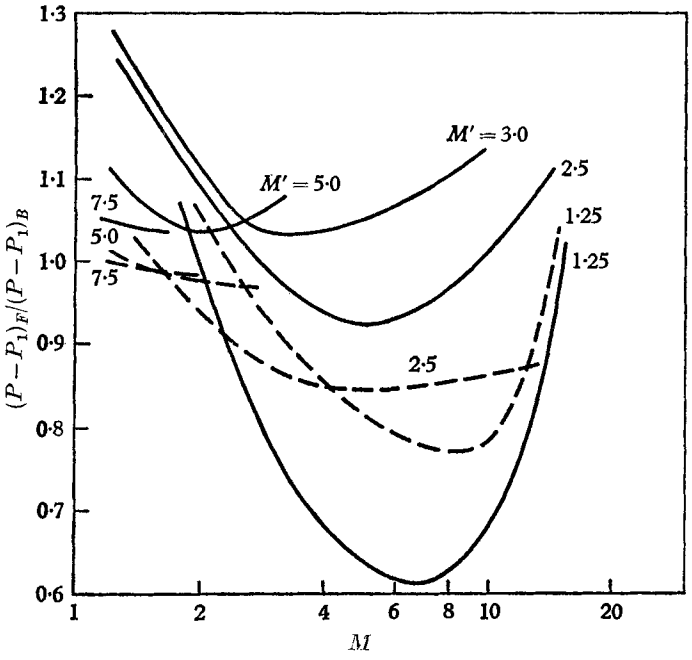

FIGURE 8. Ratio of surface transient peak to steady state pressure for different values of M and M'. – – –, Wedge; ——, cone.

with one end cut off by a plane with a cone inserted through the centre. This distribution is then magnified with time in a conical manner with the geometry at succeeding times remaining symmetrical. Figures 6 and 7 are characteristic of all the results obtained.

Figure 8 illustrates the ratio of the transient surface pressure behind the diffracted shock compared to the new steady surface pressure of region (5) for different values of M and M'. The wedge values are calculated from Smyrl (1963) and are compared to cone values obtained here. For the most part the pressure ratios of the wedge do not exceed one except for small values of M' and low and high values of M. However, in contrast to the wedge the cone values seem mostly to exceed one except for small values of M', in particular $M' = 1{\cdot}25$, where the cone values follow quite closely the trend of the wedge. By increasing M', the ratio increases until $M' > 5$, then it decreases. For constant M' the

pressure ratio first decreases then steadily increases for increasing blast shock strength; figure 8 is incomplete in some regions because the theory does not apply.

7. Conclusion

It was found that the ratio of the transient surface pressure directly behind the diffracted shock to the new steady surface pressure ranges from 1·25 to 0·6. The pressure ratio for the wedge is in general below one, although for some cases it does exceed one. This is to be expected because the wedge is a two-dimensional problem, whereas the cone is three-dimensional, and therefore they should yield characteristically different results. The results also indicate, within the limits of the analysis, that increasing the Mach number of the cone, the Mach number of the plane shock being less than 4, gives a decrease in the pressure ratio from values greater than 1·0 to values approaching 1·0 and perhaps slightly below. It appears, therefore, that for the hypersonic régime the pressure ratio is less than or equal to one. For the range of plane shock Mach number $2 < M < 10$ the maximum pressure ratio is 1·1 and there is a large variation in the value of the pressure ratio.

The author is grateful to Dr Adolph Busemann for his interest and suggestions during the course of this study and to N. Wayne Rhodus for his work in connexion with the computer programme. The continued encouragement of Dr Paul M. Chung has also been of great assistance.

REFERENCES

Bryson, A. E. & Gross, R. W. F. 1961 *J. Fluid Mech.* **10**, 1.

Busemann, A. 1943 *Luftfahrtforsch.* **20**, 105.

Chester, W. 1954 *Quart. J. Mech. Appl. Math.* **7**, 57.

Courant, R. & Friedrichs, K. O. 1948 *Supersonic Flow and Shock Waves.* New York: Interscience.

Ehlers, F. E. & Shoemaker, E. M. 1959 *J. Aero/Space Sci.* **26**, 75.

Forsythe, G. E. & Wasow, W. R. 1960 *Finite Difference Methods for Partial Differential Equations.* New York: Wiley.

Liepmann, H. W. & Roshko, A. 1956 *Elements of Gasdynamics.* New York: Wiley.

Lighthill, M. J. 1949 *Proc. Roy. Soc.* A, **198**, 454.

Ludloff, H. F. & Friedman, M. B. 1952 *J. Aero. Sci.* **19**, 425.

Miles, J. W. 1963 *Aerospace Corp. Rep.* no. TDR-269(4230-30)-1.

Miles, J. W. 1964 *Aerospace Corp. Rep.* no. TDR-269(4230-30)-5.

Smyrl, J. L. 1963 *J. Fluid Mech.* **15**, 223.

Ting, L. & Ludloff, H. F. 1952 *J. Aero Sci.* **19**, 317.

Whitham, G. B. 1957 *J. Fluid Mech.* **2**, 145.

Whitham, G. B. 1958 *J. Fluid Mech.* **4**, 337.

Whitham, G. B. 1959 *J. Fluid Mech.* **5**, 369.

r	$\frac{T_0 P'_B(x_0, r)}{r_3}$	$\frac{T_0 P_c(x_0, r)}{2r_3}$	$P'(x_0, r)$
$W = 2000$ ft./sec, $U = 9000$ ft./sec, $C_0 = 800$ ft./sec, $\gamma = 1{\cdot}4$			
0	—	—	—
0·05	2·12365	1·11742	21·809
0·1	2·00596	1·09001	18·293
0·2	1·76996	1·00313	14·026
0·3	1·53559	0·88801	11·336
0·4	1·30416	0·75611	9·3264
0·5	1·07692	0·61627	7·6744
0·6	0·85566	0·47638	6·2228
0·7	0·64347	0·34422	4·8763
0·8	0·44639	0·22818	3·5627
0·9	0·27978	0·13818	2·2120
1·0	0·17826	0·07462	Equation (21)
1·10	0·08301	0·02394	Equation (21)
1·20	0·00000	0·00000	Equation (21)
$W = 2000$ ft./sec, $U = 5000$ ft./sec, $C_0 = 800$ ft./sec, $\gamma = 1{\cdot}4$			
0·05	2·27815	1·29962	24·141
0·1	2·16220	1·27192	20·427
0·2	1·92869	1·18323	15·851
0·3	1·69525	1·06442	12·949
0·4	1·46314	0·92679	10·774
0·5	1·23355	0·77915	8·9788
0·6	1·00822	0·62942	7·3920
0·7	0·79035	0·48552	5·9075
0·8	0·58657	0·35620	4·4398
0·9	0·41593	0·25215	2·9370
1·00	0·31142	0·17044	Equation (21)
1·10	0·20999	0·09711	Equation (21)
1·20	0·10857	0·03665	Equation (21)
1·25	0·05786	0·03183	Equation (21)
1·40	0·00000	0·00000	Equation (21)
$W = 7000$ ft./sec, $U = 3000$ ft./sec, $C_0 = 1400$ ft./sec, $\gamma = 1{\cdot}4$			
0·05	4·46685	2·39388	87·610
0·1	4·22554	2·33750	73·497
0·3	3·74527	2·15866	56·477
0·3	3·27078	1·92090	45·837
0·4	2·80362	1·62704	37·957
0·5	2·34575	1·35433	31·553
0·6	1·90025	1·05766	26·023
0·7	1·47215	0·77085	21·050
0·8	1·06984	0·50683	16·54
0·9	0·69301	0·27401	Equation (21)
1·00	0·31766	0·08602	Equation (21)
1·10	0·00000	0·00000	Equation (21)

TABLE 1